Temperature Dependent Optimal Power Flow Using Combined Particle Swarm Optimization and Differential Evolution Method

Trung Minh Dao[1,2], Minh Quang Tran[1], Long Thanh Duong[3], Duy Phuong Nguyen Do[2], Nam Nhat Nguyen[1,4], and Dieu Ngoc Vo[1,4,*]

ARTICLE INFO

Article history:
Received: 2 August 2022
Revised: 12 December 2022
Accepted: 28 March 2023

Keywords:
Constriction factor
Differential evolution
Particle swarm optimization
Pseudo-gradient
Temperature dependent optimal power flow

ABSTRACT

In practice, the conductor resistance of elements in power systems is not a constant but depends on the temperature. The conventional power flow problem considering the conductor resistance as a constant may lead to not exact results, especially for the power losses. In this paper, a combined particle swarm optimization and differential evolution (CPSO-DE) method is proposed to solve the temperature dependent optimal power flow (TDOPF) problem in power systems. The considered TDOPF problem is a very large-scale and complex problem in power systems due to the consideration of the effect of temperature on the resistance of transmission lines in the conventional OPF problem. On the other hand, the proposed CPSO-DE is a powerful method suitable for solving OPF problems by utilizing the advantages of both PSO and DE algorithms to find the optimal solution. For implementing the proposed method to the TDOPF problem, the PSO algorithm with constriction factor guided by a pseudo-gradient method is first used to explore the global search space of the problem and then the DE algorithm is used to exploit the local search space of the problem to guarantee that the near optimal solution can be found. To validate the effectiveness of the proposed method for the considered problem, the IEEE 30-bus and IEEE 118-bus systems have been used for testing and the results obtained from the proposed method have been compared to those from other methods for the both conventional OPF and TDOPF problems. The test results have indicated that the proposed method can effectively solve these problems compared to other methods for the considered cases. Therefore, the proposed CPSO-DE method is a very effective method for solving the large-scale and complex TDOPF problem in power systems.

1. INTRODUCTION

The power flow analysis is an important problem in planning, expansion and state evaluation of power systems. The power flow analysis results also are used in optimal power flow, transient stability, and economy dispatch problems. Therefore, the accuracy of the power flow plays a very important part in the power system analysis and operation [1]. As the temperature changed, the resistance of conductors in transmission systems will also change accordingly. In fact, the difference of conductor resistance values in winter and summer is nearly 15% [2]. However, the temperature effect on the conductors is usually neglected in the conventional power flow problem. Therefore, conventional power flow usually results a difference compared to the practical case, especially in the total branch and system losses. For a more exact result, the temperature effect on the conductor resistance should be considered in the power flow calculation.

On the other hand, the optimal power flow (OPF) is one of the problems that use the power flow result to determine the best operating levels for generators, transformers, and shunt capacitors in power systems to minimize a specified objective while satisfying all generators, transformers, shunt capacitors, and system constraints [3]. The OPF problem is widely used in the power system operation, expansion planning, and electricity market assessment and solved by using several conventional and heuristic methods in the literature. Some conventional methods have been developed in the early decades to solve the OPF problem such as nonlinear programming (NLP) [3-7], quadratic programming (QP) [7], linear programming (LP) [8-10], Newton method and interior point method (IP) [11]. These methods have been successfully applied for solving the

[1]*Department of Power Systems, Ho Chi Minh City University of Technology (HCMUT), 268 Ly Thuong Kiet Street, District 10, Ho Chi Minh City, Vietnam*
[2]*Department of Electrical Engineering, College of Engineering Technology, Can Tho University, Can Tho City, Vietnam*
[3]*Faculty of Electrical and Electronics Technology Engineering, Industrial University of Ho Chi Minh City, Ho Chi Minh City, Vietnam*
[4]*Vietnam National University Ho Chi Minh, Linh Trung Ward, Thu Duc City, Ho Chi Minh City, Vietnam*
**Corresponding author:* Dieu Ngoc Vo; E-mail: vndieu@hcmut.edu.vn and Trung Minh Dao; Email: dmtrung.sdh21@hcmut.edu.vn.

problem with the advantages of robust and fast for obtaining the optimal solution for the problem and many of them can be used in the industrial practice. However, these methods still suffer difficulty when dealing with the OPF problem with non-convex objective functions as well as finding the global optimal solution for the large-scale OPF problem with complex constraints. Moreover, the OPF problems solved by these methods did not consider the effect of the temperature on the conductor resistance. In fact, it will be more difficult for applying these methods for solving the OPF problem considering the effect of the temperature on the conductors due to increasing the complexity and dimension of the problem.

Recently, the methods based on meta-heuristic search have been developed to overcome the disadvantages of the conventional optimization techniques and widely applied for solving different optimization problems. Several meta-heuristic search methods have been implemented to solve the OPF problem such as basic particle swarm optimization (PSO) [12], PSO with inertia weight factor (IWPSO) [13], PSO using adaptive acceleration factors and different mutation formulas (APSO) [14], weights aggregated multi-objective PSO (WAMOPSO) [15], PSO with graphics processing unit (GPU-PSO) [16], PSO with pseudo-gradient search and constriction factor (PG-CF-PSO) [17], PSO with evolving ant direction (EADPSO) [18], basic differential evolution algorithm (DE) [19, 20], modified DE (MDE) [21], moth swarm algorithm (MSA) [22], artificial bee colony algorithm (ABC) [23], evolutionary programming (EP) [24], Adaptive Real Coded Biogeography-Based Optimization (ARCBBO) [25], Grey Wolf Optimizer (GWO) [26], Krill Herd algorithm (KHA) and improved Krill Herd algorithm (IKHA) [27], tabu search algorithm (TS) [28], Gaussian bare-bones imperialist competitive algorithm (GBICA) and modified Gaussian bare-bones imperialist competitive algorithm [29], moth-flame optimization algorithm (MFO) and improved moth-flame optimization algorithm (IMFO) [30], harmony search algorithm (HSA) and fuzzy harmony search algorithm (FHSA) [31], backtracking search optimization algorithm (BSA) [32], improved colliding bodies optimization algorithm (ICBO) [33], Salp swarm optimizer (SSA) [34], fuzzy adaptive hybrid self-adaptive particle swarm optimization (FAHSPSO-DE) [35]. The MDE method in [21] has used a vector x_{best} instead of random vector x_1 in the mutation stage to improve convergence rate and the differential weight *F* value is calculated based on the current iteration. The MSA method in [22] is inspired by the orientation of moths towards the light source and applied to achieve the fuel cost in a 30-bus system. The ABC method [23] is inspired by the bees looking for food based on three types of bees including employed bees, onlooker bees, and scout bees. The EP method in [24] uses the mutation, competition, and selection mechanisms to achieve the global best solution. The ARCBBO [25] uses the improved mutation mechanism to enhance the convergence rate for solving the OPF problem. The GWO method [26] is based on four types of wolves in a wolf pack those are α, β, δ and ω and the pack activities which are hunting, searching for prey, encircling prey, and attacking prey are implemented on the algorithm. The GWO method has been successfully used to solve OPF problem in 30 and 118 bus systems. The KHA method and its improved version, namely IKHA, are proposed in [27] and have successfully solved the OPF problem with different objective functions on 30, 57 and 118 bus systems. On the other hand, some other studies have also consider other factors affecting to the OPF problem such as IPSO applied for solving the OPF problem with FACTS devices [36] and Equilibrium optimizer (EO) method for solving the OPF problem considering wind power integrated in the system [37]. These problem is more complex than the original OPF problem due to considering other factors. In general, the advantages of meta-heuristic search methods for solving optimization problems are easy for implementation, able to deal with different types of complex optimization problems, and able to find the near-optimum solution. However, these methods may still suffer local optima due to their initialization and parameter dependent. Moreover, the OPF problem solved by the mentioned methods did not consider the effect of the temperature on the conductor resistance in power systems.

In recent studies, the temperature dependent of transmission lines in power systems has been considered in the power flow problem [38-40]. In these studies, the temperature of transmission lines is considered as a control variable vector which will be included in the calculation. Consequently, the power flow becomes a more complex and larger scale problem compared to the conventional power problem. However, as the temperature dependent power flow problem will lead to a more exact result on the power loss calculation in power systems. Therefore, the temperature dependent power flow problem has become a basis for further studies in power systems. One of the optimization problems in power systems considering the temperature dependent of transmission lines which have attracted the attention of researchers recently is the temperature dependent optimal power flow (TDOPF) [41-46]. In [41], the authors have implemented a simplified interior point for dealing with the TDOPF and decoupled TDOPF problems for large-scale systems up to 3012 buses. However, the obtained results from this study are only verified to those from the conventional OPF problem. The gbest-guided artificial bee colony (GABC) algorithm [43] has been proposed for solving the TDOPF problem and test on the IEEE 30 bus system and large-scale Polish systems. Similar to the study in [41], the results obtained in this study are also only verified by comparing to those from the conventional OPF problem. In another study, a sine cosine algorithm (SCA) has been implemented to solve the TDOPF problem [44]. This study only considered the IEEE 30 bus

system and also verified the obtained result via comparing to that from the conventional OPF problem. The chaotic whale optimization algorithm (CWOA) has been also proposed for solving the TDOPF problem and applied to the IEEE 30 bus and large-scale Polish systems. The results comparisons have indicated that the CWOA is more effective than the GABC in terms of the fuel cost and power loss for the test cases. The TDOPF problem with the integration of distributed generations has been solved by the quantum-behaved particle swarm optimization (QPSO) as in [44]. Generally, the TDOPF problem has started attracting the attention of researchers recently due to its ability to provide an exact solution to the practice.

Among several meta-heuristic search methods developed for solving different optimization problems, PSO and DE are the most widely used methods in the literature with many their variants. The advantages of the PSO method are simple, fast calculation, easy to combine with other methods, and able to deal with large-scale problems while the advantages of the DE method are good at exploration with diversification and able to converge to the global minimum. However, both the methods have also disadvantaged like many other meta-heuristic search methods. The PSO may suffer a local optimum due to its premature convergence meanwhile the DE method requires a parameter tuning and may not be stable convergence for large-scale optimization problems. Therefore, their improved versions are continually developed to enhance their performance for effective dealing different optimization problems. In this paper, a combined PSO and DE (CPSO-DE) method is proposed to solve the TDOPF problem. The proposed method can overcome the disadvantages of the both for effectively dealing with large-scale and complexity-constrained optimization problems where the PSO method is used to explore the search space of the problem for the global search and then the DE is used to exploit the local search. By using the combination, the proposed method can effectively solve the large-scale with complex constraints of the TDOPF problem. The proposed CPSO-DE has been validated on the benchmark systems such as the IEEE 30-bus and IEEE 118-bus systems by comparing the obtained results to those from other methods in the literature as well as the PSO and DE methods.

The main contributions of this paper are as follows:

- Development of a combined method of PSO and DE for effectively dealing with large-scale optimization problems with complex constraints.
- Implementation of the proposed CPSO-DE method for solving the very large-scale and complexity-constrained TDOPF problem.
- The proposed method has been verified on test systems including the IEEE 30 and 118 bus systems.
- The test results obatined from the proposed method have been validated via comparing to those obtained from the mature optimization methods in the literature as well as the PSO and DE methods.
- The result comparisons have indicated that the proposed method is more effective than the compared methods. Thus, the proposed CPSO-DE can effectively deal with the TDOPF problem.

The remaining parts of the paper are organized as follows. Section 2 presents the mathematical model of the TDOPF problem, the proposed CPSO-DE method and implementation to the TDOPF problem are introduced in Section 3, the simulation results are provided in Section 4 and finally the conclusion is given.

2. FORMULATION OF TEMPERATURE DEPENDENT OPTIMAL POWER FLOW PROBLEM

The objective of temperature dependent optimal power flow (TDOPF) problem is to minimize a specified objective while satisfying a set of equality and inequality constraints. Similar to the conventional OPF problem, the mathematical model of the TDOPF problem can be formulated as follows:

$$\text{Minimize } f(x,u) \tag{1}$$

subject to following constraints:

$$g(x,u) = 0 \tag{2}$$

$$h(x,u) \leq 0 \tag{3}$$

where, f is the objective function of the problem, x is the vector of dependent (state) variables, u is the vector of independent (control) variables, g is the set of equality constraints and h is the set of inequality constraints.

The vector of control variables u for the OPF problem including the power outputs at generation buses excluding the slack bus, voltage at generation buses, reactive power at buses with shunt capacitors, and step ratio in the on-load tap changer of transformers can be described as follows:

$$u^T = [P_{g2}, \dots, P_{Ng}, V_{g1}, \dots, V_{N_g}, Q_1, \dots, Q_{N_c}, T_1, \dots, T_{N_t}] \tag{4}$$

where, P_g is the active power of generator, V_g is the voltage at generator bus, Q is the reactive power of compensator, T is the tap ratio of transformer; N_g, N_c, and N_t are the number of generators, number of shunt compensators and number of transformers.

The vector of state variables x may be represented by:

$$x^T = [P_{gslack}, Q_{g1}, \dots, Q_{Ng}, V_1, \dots, V_{N_{PQ}}, S_1, \dots, S_{N_{TL}}] \tag{5}$$

where, P_{gslack} is the active power output of slack bus generator, Q_g is the reative power output at generator bus, V is the voltage at load bus, S is the loading of transmission line; N_{PQ} and N_{TL} are number of load buses and number of transmission lines.

2.1 Objective function

In this paper, total fuel cost is used as objective function and can be described as:

$$Min\ f(x,u) = \sum_{k=1}^{N_g} \left(a_k + b_k P_{gk} + c_k P_{gk}^2\right) \quad (6)$$

where, $f(x,u)$ is the total cost of all generators, P_{gk} is the active power output of k^{th} generator; a_k, b_k and c_k are the cost coefficients of kth generator.

2.2 The equality and inequality constraints

All the constraints of the TDOPF problem are shown as below:

1) Power balance for each bus and heat balance for each branch

$$P_{gk} - P_{dk} - V_k \sum_{i=1}^{Nbus} \begin{matrix}(V_i(G_{ki}(T).cos(\delta_k - \delta_i) \\ +B_{ki}(T).sin\ (\delta_k - \delta_i))\end{matrix} = 0 \quad (7)$$

$$Q_{gk} - Q_{dk} - V_k \sum_{i=1}^{Nbus} \begin{matrix}(V_i(G_{ki}(T).sin(\delta_k - \delta_i) \\ -B_{ki}(T).cos\ (\delta_k - \delta_i))\end{matrix} = 0 \quad (8)$$

$$T_{ki} - \Big(T_{amb} + R_{\theta,ki}.(g_{ki}(T).(V_k^2 + V_i^2) - 2g_{ki}(T).V_k V_i\, cos(\delta_k - \delta_i))\Big) = 0 \quad (9)$$

2) Real and reactive power limit at generation buses

$$P_{gk}^{min} \le P_{gk} \le P_{gk}^{max} \quad k = 1, \dots N_g \quad (10)$$

$$Q_{gk}^{min} \le Q_{gk} \le Q_{gk}^{max} \quad k = 1, \dots N_g \quad (11)$$

3) Voltage limit at generation buses

$$V_{gk}^{min} \le V_{gk} \le V_{gk}^{max} \quad k = 1, \dots N_g \quad (12)$$

4) Reactive power limit of shunt capacitor

$$Q_{ck}^{min} \le Q_{ck} \le Q_{shk}^{max} \quad k = 1, \dots N_c \quad (13)$$

5) Transformer tap changer limit

$$T_k^{min} \le T_k \le T_k^{max} \quad k = 1, \dots N_t \quad (14)$$

6) Voltage limit at load buses

$$V_{lk}^{min} \le V_{lk} \le V_{lk}^{max} \quad k = 1, \dots N_{PQ} \quad (15)$$

7) Power limit on transmission lines

$$S_k \le S_k^{max}, k = 1, \dots N_{TL} \quad (16)$$

where, P_{gk} is the active power output of k^{th} generator, V_{gk} is the voltage of k^{th} generator bus, T_k is the tap ratio of k^{th} transformer, Q_{ck} is the reactive power output of k^{th} shunt compensator, Q_{gk} is the reactive power output of k^{th} generator, V_{Lk} is the voltage of k^{th} load bus, and S_k is the rating of k^{th} transmission line.

3. IMPLEMENTATION OF CPSO-DE FOR THE PROBLEM

3.1 Temperature dependent power flow problem

In power systems, all elements have resistance which are actually non-linear ones, that means the resistance in the elements will vary following the change of temperature. The resistance of conductors is a function of temperature and described by [47- 48]:

$$R = R_{ref} * \frac{T + T_f}{T_{Ref} + T_f} \quad (17)$$

in which, R is conductor resistance at T^0C, T is conductor temperature, R_{ref} is conductor resistance at reference temperature, T_{Ref} is the reference temperature, T_f is the temperature constant.

The thermal modelling of power system elements is given in [1-2, 49]. In temperature dependent power flow, it is assumed that power system is operating at steady state. Also, TDPF has modifications in state vector, mismatch equations and Jacobian matrix. Besides voltage V and voltage angle δ, TDPF has an additional state variable which is a set of branch temperature T. Like V, T is expressed in per – unit relative to a base quantity. Therefore, state vector in TDPF can be represented as:

$$x = \begin{bmatrix}\delta \\ V \\ T\end{bmatrix} \quad (18)$$

In addition to real power mismatch equations and reactive power mismatch equations, TDPF also requires temperature mismatch equations to calculate the system state. These mismatch equations are given as follows [50]:

$$\Delta P_i = \left(P_{gen,i} - P_{load,i}\right) - P_i(\delta, V, T) \quad (19)$$

$$\Delta Q_i = \left(Q_{gen,i} - Q_{load,i}\right) - Q_i(\delta, V, T) \quad (20)$$

$$\Delta H_{ij} = 0 - H_{ij}(\delta, V, T) \quad (21)$$

Due to the additional state vector, the Jacobian matrix is modified as follows [50]:

$$J(\delta, |V|, T) = \begin{bmatrix} \frac{\partial P}{\partial \delta} & \frac{\partial P}{\partial |V|} & \frac{\partial P}{\partial T} \\ \frac{\partial Q}{\partial \delta} & \frac{\partial Q}{\partial |V|} & \frac{\partial Q}{\partial T} \\ \frac{\partial H}{\partial \delta} & \frac{\partial H}{\partial |V|} & \frac{\partial H}{\partial T} \end{bmatrix} \quad (22)$$

3.2 Constraint handling method

It is worth to mention that the control variables are self-constrained. The inequality constraints P_{gslack}, V_L, Q_g, and S can be incorporated in the objective function as quadratic penalty terms (penalty functions). Therefore, the objective function can be augmented as:

$$\begin{aligned} \text{Min} \quad F(x,u) = & \left(\sum_{k=1}^{N_g} a_k \times P_{gk}^2 + b_k \times P_{gk} + c_k\right) + \lambda_1 \left(P_{glask} - P_{gslack}^{lim}\right)^2 \\ & + \left(\lambda_2 \sum_{k=1}^{N_g} \left(Q_{gk} - Q_{gk}^{lim}\right)^2\right) \\ & + \left(\lambda_3 \sum_{k=1}^{N_{PQ}} \left(V_{lk} - V_{lk}^{lim}\right)^2\right) \\ & + \left(\lambda_4 \sum_{k=1}^{N_T} \left(S_k - S_k^{lim}\right)^2\right) \end{aligned} \tag{23}$$

where, P_{gslack}^{lim} is the active power limit of slack bus generator, Q_{gk}^{lim} is the reactive power limit of kth generator, V_{lk}^{lim} is the upper and lower voltage limit of k^{th} load bus, S_k^{lim} is the rating of kth tranmission line, λ_1, λ_2, λ_3 and λ_4 are penalty factors. The objective of OPF problem is to minimize the objective function while all constraints are satisfied. Therefore, the penalty should be zero. To prevent constraints from violation, penalty factors should be precisely chosen. Too large values will lead to a slow convergence rate and in the worst case, global minimum can't be found. On the contrary, if values are too small, constraints can easily be violated.

3.3 The proposed CPSO-DE method

Differential evolution (DE) and particle swarm optimization (PSO) are two famous and powerful methods among swarm intelligence algorithms for solving different optimization problems.

The PSO method [51] is an optimizatimal method to optimize a problem by iteratively improve a swarm of candidate solutions regarding to a given measure of quality. The method solves an optimization problem by using a population set of candidate solutions which are aclled paticles to find the optimal solution by moving these particles in the search-space of the problem based on the simple mathematical formulae preresented by the position and velocity of these particles. The movement of each paticle is affected by its local best position and it is also guided toward the best position known before in the search-space of the problem, which will be updated as long as better positions are found by other particles. This mechanism is expected to move the population swarm moving toward the best global solution of the problem. In fact, the PSO method is a metaheuristic as it makes few or no assumptions about the optimal problem being considered and it can also search in very large spaces of candidate solutions. Moreover, the PSO method does not also use the gradient of the optimal problem being considered, this means that the PSO method does not require the optimal problem to be differentiable similar to the classic optimal methods such as gradient descent or quasi-newton method. Although it has been successfully used for solving the continuous optimization problem, the PSO method is easily getting stuck in local optimal due to the loss of population diversity.

On the other hand, the DE method introduced in 1997 by Storn and Price [52] is also a effective method for dealing with optimization problems by iteratively improving the quality of a candidate solution. The DE method can finding the optimal solution of a problem via maintaining a candidate population of solutions as well as creating new candidate population of solutions by combining with the existing ones, and then whichever candidate solution has the better quality will be updated for the next step. By this way, the optimization problem can be easily solved merely by comparing the measure of quality from the candidate solutions. In this method, the gradient is also not needed. The DE algorithm has some advantages those are its ability to maintain the diversity of population as well as to explore the local search. However, it has no mechanism to memorize the previous process as well as uses the global information about the search space in the problem being considered, thus it easily gets trapped in local optima, leading to a waste of computing power. Therefore, the differential information can be helpful for the search ability of this method, but it may also lead to instability of some solutions.

Considering the advantages and disadvantages of DE and PSO, a combined pseudo-gradient based PSO with constriction factor and the DE method is proposed for solving the security-constrained OPF problem [40] which aim to achieve both fast convergence speed and efficient global optimization. PGPSO-DE has proved to be an effective algorithm for solving OPF problem in small as well as large-scale systems. As mentioned, solving the TDOPF problem might be challenging since it includes the temperature effect into calculation. Therefore, some improvements are implemented in the original PGPSO-DE algorithm to make it more effective for dealing with the complex TDOPF problem.

The main steps of the proposed CPSO-DE method for an optimization problem is as follows:

- *Initialization phase*

In this step, position and velocity of each particle are randomly selected by uniform probability:

$$x_{i,d}^0 = x_d^{min} + rand(0,1)(x_d^{max} - x_d^{min}) \tag{24}$$

$$v_{i,d}^0 = v_d^{min} + rand(0,1)(v_d^{max} - v_d^{min}) \tag{25}$$

$$i = 1, \ldots, N_p \text{ and } d = 1, \ldots, D$$

where, N_p is the number of particles, D is the number of control variables, x_i and v_i are the position and velocity of ith particle, x_d^{max} and x_d^{min} are the upper and lower limit of dth control variable, v_d^{max} and v_d^{min} are the maximum and minimum velocity which are calculated as follows:

$$v_d^{max} = R(x_d^{max} - x_d^{min}) \quad (26)$$

$$v_d^{min} = -v_d^{max} \quad (27)$$

where, R is the velocity scale factor.

• *Applying PSO mechanism to generate the first generation:*

At this step, velocity and position of each particle are achieved using PSO algorithm:

$$v_{id}^{k+1} = \omega . v_{id}^{k} + c_1 . rand_1(0,1)\left(pbest_i^k - x_{id}^k\right) + c_2 . rand_2(0,1)(gbest - x_{id}^k) \quad (28)$$

$$x_{id}^{k+1} = x_{id}^{k} + v_{id}^{k+1} \quad (29)$$

where, k is the iteration, c_1 and c_2 are the acceleration constants, $pbest_i$ is the best known position of i^{th} particle, ω is the inertia weight, $rand_1$ and $rand_2$ are two random numbers within [0,1], $gbest$ is the best known position of population. If velocity and position are outside the bounds, they will be set equal to the bounds they violate:

$$v_{id}^{k+1} = \begin{cases} v_d^{max} & if\ v_{id}^{k+1} > v_d^{max} \\ v_d^{min} & if\ v_{id}^{k+1} < v_d^{min} \end{cases} \quad (30)$$

$$x_{id}^{k+1} = \begin{cases} x_d^{max} & if\ x_{id}^{k+1} > x_d^{max} \\ x_d^{min} & if\ x_{id}^{k+1} < x_d^{min} \end{cases} \quad (31)$$

• *Applying three DE mechanisms to generate the second generation*

* *Mutation process*

The mutation strategy is employed on first generation:

$$x_{id}'^{k+1} = x_{r1d}^{k+1} + F(x_{r2d}^{k+1} - x_{r3d}^{k+1}) \quad (32)$$

where, r_1, r_2, r_3 are three random particles that are different from particle i, F is the differential weight. If positions are outside the bound, they will be set similarly to (31).

* *Crossover process*

At this step, the crossover operator is performed to generate second generation:

$$x_{id}''^{k+1} = \begin{cases} x_{id}'^{k+1} & if\ rand(0,1) \le CR\ or\ d = D_{rand} \\ x^{k+1} & otherwise \end{cases} \quad (33)$$

where, CR is the crossover rate, D_{rand} is a random control variable. Then the fitness value will be calculated.

* *Selection process*

The selection operator is utilized to choose a better position between x_{id}^{k+1} and $x_{id}''^{k+1}$ based on fitness values. The selection criterion may be expressed as follows:

$$x_{id}^{k+1} = \begin{cases} x_{id}''^{k+1} & if\ f(x_{id}''^{k+1}) \le f(x_{id}^{k+1}) \\ x_{id}^{k+1} & otherwise \end{cases} \quad (34)$$

3.4 Implementation of CPSO-DE method for the TDOPF problem

The proposed CPSO-DE method is implemented for solving the temperature dependent optimal power flow problem is shown in Figure 1.

4. SIMULATION RESULTS

In this paper, the quadratic cost function is selected as objective function. CPSO-DE algorithm will be applied to solve conventional OPF and TDOPF problem in the IEEE 30 bus and 118 bus system.

For TDOPF simulation, the rated temperature rise values, which directly affect the thermal resistances and temperature of transmission lines (17) will be increased with a step of 5^0C and the fuel cost relative to each rated temperature rise value will be compared to those from GABC [43].

4.1 The IEEE 30 bus system

4.1.1 Conventional optimal power flow

The IEEE 30 bus system has six generators at bus 1, 2, 5, 8, 11 and 13; forty-one transmission lines; four tap changing transformers and nine shunt compensators at bus 10, 12, 15, 17, 20, 21, 23, 24 and 29. The upper and lower limits of tap changing transformers are 1.1 and 0.9 p.u. respectively. The load bus upper and lower voltage limits are 1.05 and 0.95 p.u. The PV bus upper and lower voltage limits are 1.1 and 0.9 p.u. Base power is selected as 100 MVA. Bus data, line data, generator cost data, limit of control variables and state variables are taken from Matpower 7.1 [53]. Maximum number of iterations and number of particles are selected as 100 and 50 respectively. All CPSO-DE, DE and PSO parameters are given in Table A.1 in Appendix. Fifty successful runs are obtained using CPSO-DE, DE and PSO and results are shown in Figure 2. The best cost, worst cost, mean cost, standard deviation and success rate of CPSO-DE, DE, PSO are given in Table 1.

Table 1. Fuel cost obtained from the conventional OPF for the IEEE 30 bus system

Algorithm	Best cost	Worst cost	Mean cost	Standard deviation	Success rate
CPSO-DE	800.4353	801.7535	801.1814	0.4483	100%
DE	800.6882	809.9819	801.7580	2.1034	100%
PSO	800.7292	804.8902	801.8953	0.94	98.04%

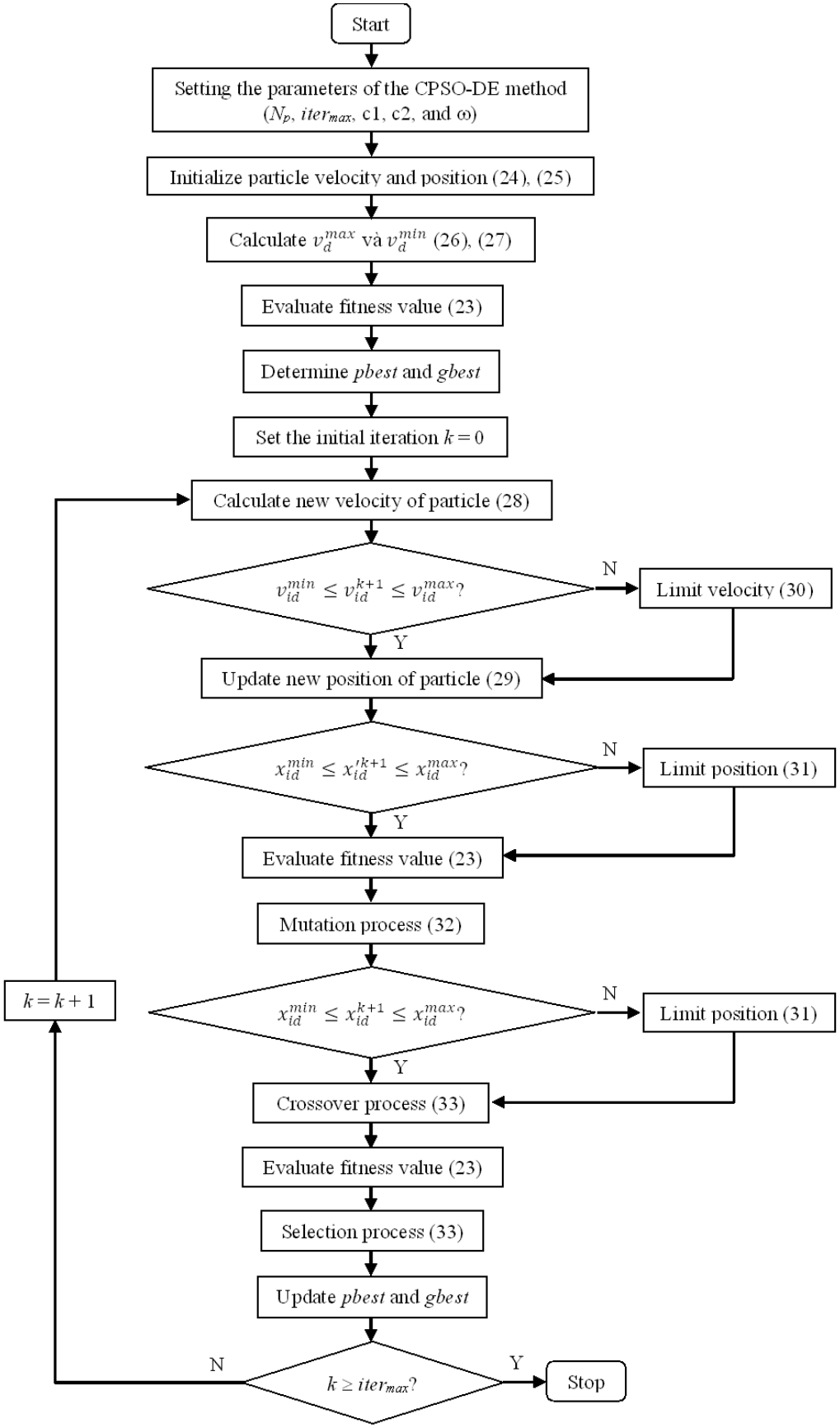

Fig. 1. Flow chart of CPSO-DE algorithm for solving the TDOPF problem.

The best cost obtained from CPSO-DE is 800.4353 ($/h). Some papers get better cost (under 800 $/h) but either load bus voltage limit or reactive power source limit is set higher. The comparison of CPSO-DE algorithm with other algorithms is shown in Table 2. All control variables of the best run are provided in Table A.2 of the Appendix. The convergence characteristic of the CPSO-DE algorithm compared to that from DE and PSO is shown in Figure 3. It can be seen that the CPSO-DE can achieve good fuel cost compared to other recent algorithms. When compared with original DE and PSO, best cost obtained from CPSO-DE is better with lower or equal success rate.

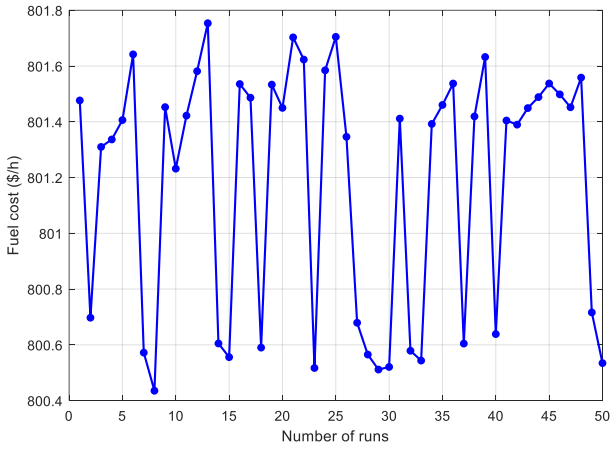

Fig. 2. Fuel cost obtained from 50 runs on the IEEE 30 bus system.

Table 2. Comparison of minimum costs obtained for the IEEE 30 bus system

Algorithm	Min fuel cost ($/h)	Algorithm	Min fuel cost ($/h)
CPSO-DE	800.4353	RCBBO [25]	800.8703
EADPSO [15]	800.2276*	GWO [26]	801.41
GPU-PSO [17]	800.53	KHA [27]	801.4675
MDE [21]	802.376	IKHA [27]	800.4143
MSA [22]	800.5099	TS [28]	802.29
ABC [23]	800.66	GBICA [29]	801.1513
GABC [43]	800.440	MGBICA [29]	801.1409
EP [24]	802.62	IMFO [30]	800.3848
ARCBBO [25]	800.5159	MFO [30]	800.6206

* Not applicable or violated solution

4.1.2 Temperature dependent optimal power flow

Base temperature and ambient temperature are selected as 100^0C and 25^0C. Changes in fuel cost and power loss obtained from CPSO-DE, DE and PSO with different temperature rises are given in Table 3, Table 4, and Table 5.

Fig 4 shows convergence characteristic of CPSO-DE algorithm compared to DE and PSO for 25^0C temperature rise. Fig 5 shows changes in fuel cost and power loss with different rated temperature rise values.

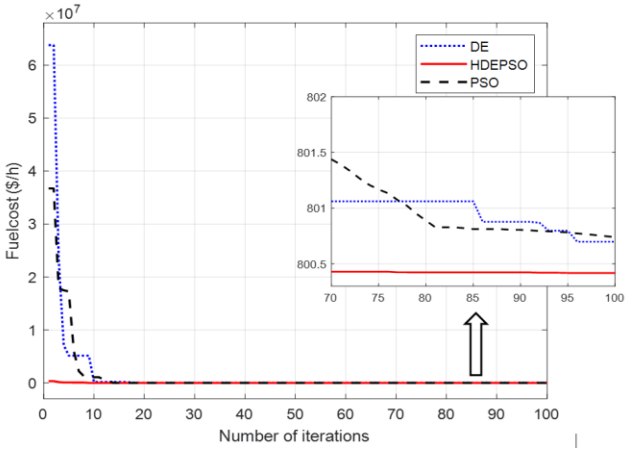

Fig. 3. Convergence characteristic of solution methods for the IEEE 30 bus system.

All control variables for 25^0C temperature rise TDOPF are given in Table A.3. Changes in transmission line resistance for 25^0C temperature rise TDOPF are given in Table A.4.

Table 3. The changes in fuel cost and power loss obtained from the CPS-DE with different temperature rise values in the IEEE 30 bus system

$T_{RatedRise}$	CPSO-DE				
	Best cost ($)	Worst cost ($)	Average cost ($)	Standard deviation	Success rate (%)
0	799.8645	801.1151	799.9788	0.1805	96.15
5	800.0937	801.9153	801.4722	0.5090	98.04
10	800.2781	802.6343	801.7335	0.5050	98.04
15	800.4430	802.4918	801.9216	0.5081	94.34
20	800.6130	802.5384	802.1245	0.5135	98.04
25	800.8220	801.2235	800.9529	0.0907	100
30	800.9373	803.1326	802.4740	0.5036	92.59
35	801.1429	803.2672	802.6902	0.5055	92.59
40	801.2721	803.6831	802.8831	0.5095	98.04
45	801.4604	803.6515	803.0187	0.5347	98.04
50	801.6438	803.5469	802.4721	0.7595	100

For a fair comparison with [24], a different TDOPF simulation version in which maximum load bus voltage limit is set to 1.06 is performed to prove the effectiveness of CPSO-DE algorithm. Fuel cost and power loss with different temperature rises are compared to those obtained

from [24] and shown in Table 6. It is clear that fuel cost and power loss values obtained from CPSO-DE in different temperature rise are equal to values obtained from GABC algorithm in [24].

Table 4. The changes in fuel cost and power loss obtained from the DE method with different temperature rise values in the IEEE 30 bus system

$T_{RatedRise}$	DE				
	Best cost	Worst cost	Average cost	Standard deviation	Success rate (%)
0	800.0460	854.3342	803.6966	9.9702	98.04
5	800.3272	854.4943	802.5606	7.8815	100
10	800.3909	802.9909	801.2025	0.7778	98.04
15	800.7552	816.8187	802.6462	3.8894	94.34
20	800.7764	802.4606	801.4685	0.4706	96.15
25	801.0791	853.3587	805.9503	11.9353	98.04
30	801.1942	857.8659	804.9678	12.4828	100
35	801.3709	821.3207	803.0891	4.4110	92.59
40	801.7318	861.6661	807.9160	17.3366	96.15
45	801.8348	824.4426	804.6547	6.9905	92.59
50	801.7628	824.8126	803.7472	4.6633	100

Table 5. The changes in fuel cost and power loss obtained from the PSO method with different temperature rise values in the IEEE 30 bus system

$T_{RatedRise}$	PSO				
	Best cost	Worst cost	Average cost	Standard deviation	Success rate (%)
0	800.0200	803.6747	801.3373	1.0572	100
5	800.3159	806.2028	802.5404	1.2602	100
10	800.5849	811.6553	802.7386	1.7888	100
15	800.8228	806.3119	802.6954	1.2048	98.04
20	801.0740	806.63	802.9475	1.0639	98.04
25	801.1638	808.9018	803.2543	1.6092	96.15
30	801.3076	806.6973	803.3267	1.1784	94.34
35	801.4624	803.7264	807.0175	1.0954	98.04
40	801.5847	807.9979	803.9199	1.3565	96.15
45	801.9010	805.7534	803.1781	0.4777	100
50	801.7784	807.9800	803.5424	1.2274	100

Table 6. Comparison of the changes in fuel cost and power loss for the IEEE bus system

$T_{RatedRise}$	CPSO-DE		GABC [43]	
	Best cost	Total power loss	Best cost	Total power loss
0	799.8645	8.8296	800.0627	8.9120
5	800.0937	8.9033	800.2598	8.9712
10	800.2781	8.9632	800.4531	9.0293
15	800.4430	8.9935	800.6429	9.0863
20	800.6130	9.0246	800.8292	9.1422
25	800.8220	9.0237	801.0123	9.1972
30	800.9373	9.0435	801.1922	9.2512
35	801.1429	9.1084	801.3690	9.3042
40	801.2721	9.1511	801.5429	9.3564
45	801.4604	9.1541	801.7139	9.4077
50	801.6438	9.2579	801.8822	9.4582

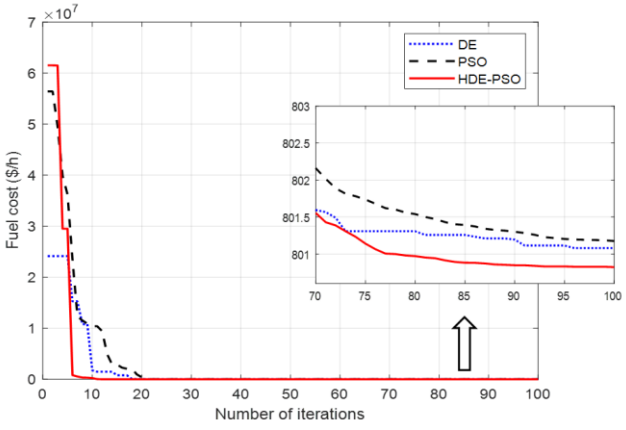

Fig. 4. The convergence characteristic of solution methods for the fuel cost at 25^{0}C rated temperature rise for the IEEE 30 bus system.

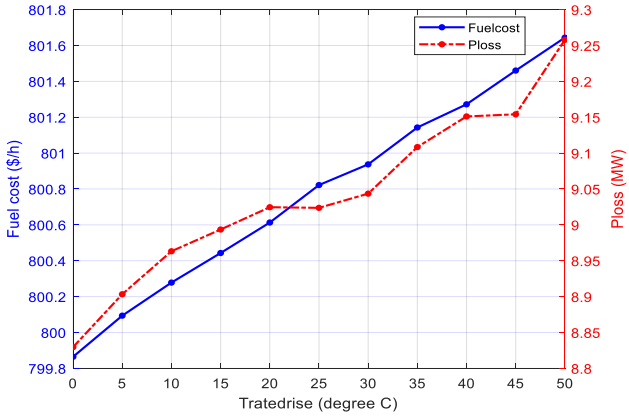

Fig. 5. The changes in fuel cost and power with different rated temperature rise values in the IEEE 30 bus system.

4.2 The IEEE 118 bus system

4.2.1 Conventional optimal power flow

The IEEE 118 bus system has 54 generators, 9 transformers, 14 shunt compensators at bus 5, 34, 37, 44, 45, 46, 48, 74, 79, 82, 83, 105, 107 and 110. The upper and lower limits of tap changing transformers are 1.1 and 0.9 p.u. The load bus upper and lower voltage limits are 1.06 and 0.94 p.u. The PV bus upper and lower voltage limits are 1.1 and 0.9 p.u. Base power is selected as 100 MVA. Bus data, line data, generator cost data, limits of control variables and state variables are taken from Matpower 7.1 [53]. All the CPSO-DE, DE and PSO parameters are given in Table A.5. Twenty success runs are performed using CPSO-DE algorithm and results are shown in Figure 6. Best cost, worst cost, mean cost, standard deviation and success rate compared to DE and PSO are given in Table 7.

Table 7. The fuel cost obtained from conventional OPF for the IEEE 118 bus system

Algorithm	CPSO-DE	DE	PSO
Best cost ($/h)	129796.169	7.736e7*	137988.546
Worst cost ($/h	147981.848	-	157209.027
Mean cost ($/h)	141190.872	-	143286.032
Standard deviation	5459.726	-	5477.647
Success rate (%)	95.23	0	86.95

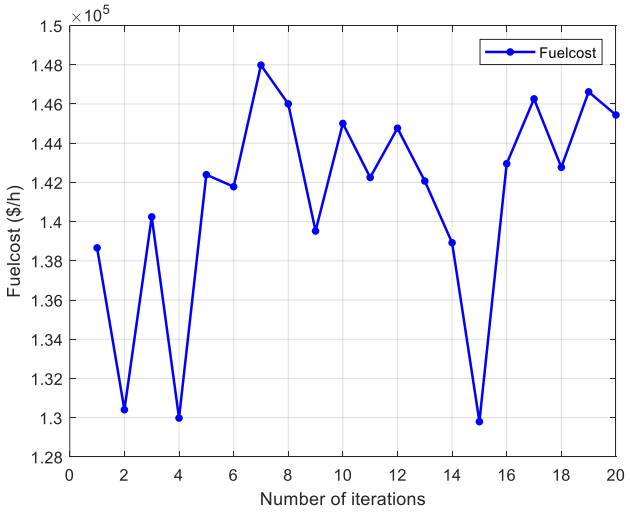

Fig. 6. The fuel cost obtained by the CPSO-DE method from 20 runs for the IEEE 118 bus system.

The best cost obtained is 129796.169 ($/h). All control variables of the best run are provided in Table A.6. Convergence characteristic of CPSO-DE algorithm compared to DE and PSO is shown in Figure 7. Also, the comparison of CPSO-DE algorithm with other algorithms is shown in Table 8.

The best cost obtained from CPSO-DE algorithm (129796.169 $/h) is equal to recently published algorithms. When compared to DE and PSO, CPSO-DE has better performance. Basic DE struggles with large scale system (as seen in Table 7) and cannot converge. Although PSO can converge and find optimal fuel cost, the value is higher than CPSO-DE.

Table 8. Comparison of minimum cost for the IEEE 118 bus system

Algorithm	Min fuel cost ($/h)	Algorithm	Min fuel cost ($/h)
CPSO-DE	129796.169	IMFO [30]	131,820
PG-CF-PSO [16]	145,520.01	HSA [31]	132,138.3
MSA [22]	129,640.7191	FHSA [31]	132,319.6
MDE [21]	130,444.5728	BSA [32]	135,333.4743
MFO [30]	129,708.0821	ICBO [33]	135,121.5704
IKHA [27]	131,427.2636	SSA [34]	129,675.0
KHA [27]	136,051.9664	FAHSPSO-DE [35]	129,519.38

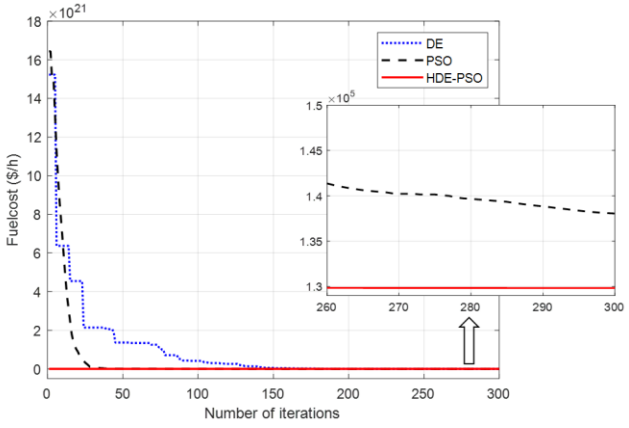

Fig. 7. The convergence characteristic of fuel cost for the IEEE 118 bus system.

4.2.2 Temperature dependent optimal power flow

Changes in fuel cost and power loss with different temperature rise values are given in Table 9. Fig 8 shows convergence characteristic of CPSO-DE algorithm compared to DE and PSO for 25^{0}C temperature rise. Fig 9 shows changes in fuel cost and power loss with different rated temperature rise values

All control variables for 25^{0}C temperature rise TDOPF are given in Table A.7. Changes in transmission line resistance for 25 ^{0}C temperature rise TDOPF are given in Table A.8.

Table 9. The changes in fuel cost and power loss by the CPSO-DE method with different temperature rises for the IEEE 118 bus system

$T_{RatedRise}$	Best cost ($/h)	Total power loss (MW)
5	129926.0610	83.3381
10	129944.2022	83.5589
15	129962.8933	84.2619
20	129966.1416	84.3649
25	129960.3155	84.1887
30	129970.7443	84.3962
35	130035.8744	86.0553
40	130056.3034	86.6652
45	130071.1035	86.6945
50	130082.9944	87.2156

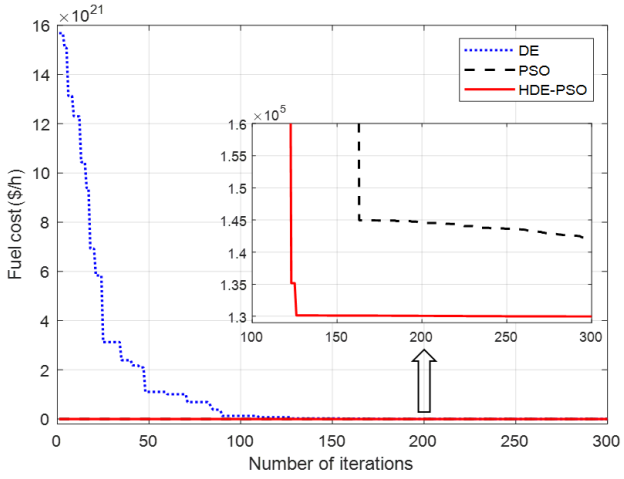

Fig. 8. The convergence characteristic of fuel cost at 25^{0}C rated temperature rise for the IEEE 118 bus system.

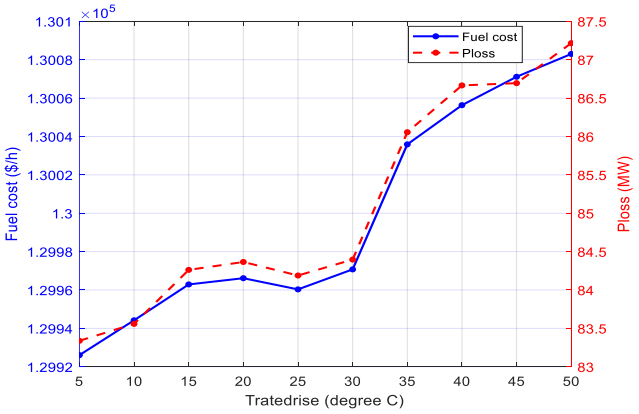

Fig. 9. The changes in fuel cost and power with different rated temperature rise values by the CPSO-DE method for the IEEE 118 bus system.

According to Table A.4, when temperature effect is included (25^{0}C rated temperature rise) in the IEEE 30 bus system, maximum relative error in branch resistance is 6.42% (line 1-2). Also fuel cost and power loss increase when rated temperature rise value increase, approximately 0.0051% increase in cost per temperature rise and 0.0905% increase in power loss per temperature rise.

In the IEEE 118 bus system, maximum relative error in branch resistance for 25^{0}C rise is considerably large (5.86%, Table A.8, line 9-10). Fuel cost and power loss increase per temperature rise are 0.22% and 4.85% respectively.

Beside the increases of fuel cost and power loss, the temperature effect has also a huge impact on the power output of generators. More specifically, if temperature effect is not included, lower cost generator tends to generate more power than higher cost ones. For example, in the IEEE 30 bus system, the slack bus generator which has the lowest cost generated the most power of all generators (177.1821 MW). But when temperature effect is considered, for example 25^{0}C rise, the lowest cost generator cannot generate as much power (175.9398 MW) because it will make the temperature of branches connecting to that generator bus rise. This results in increase in those branches resistance and power losses, so power need to be generated goes up and causes the increase in generation cost. Therefore, in TDOPF, power of all generators should suitably be distributed to minimize the generation cost.

5. CONCLUSION

In this paper, the mathematical model of the temperature dependent optimal power flow problem has been presented and the combined particle swarm optimization and differential evolution method has been implemented to solve this problem. The considered temperature dependent optimal power flow problem is very a very large-scale and complex one with the integrated of the temperature of transmission lines, leading to a big challenge for solution methods. The proposed method for dealing with the problem is a combined particle swarm optimization and differential evolution which has utilizes the advantages of each component method to find the optimal solution for the problem. The proposed method for the problem has been tested on the IEEE 30 and 118 bus systems and the obtained results have been validated via comparing to those from other methods in the literature. The result comparison has indicated that the proposed combined particle swarm optimization and differential evolution method can deal with the complex and large-scale temperature dependent optimal power flow problem in power systems.

ACKNOWLEDGMENT

This research is funded by Vietnam National University HoChiMinh City (VNU-HCM) under grant number C2021-20-14.

REFERENCES

[1] Prabha, K. 1994. Power system stability and control. New York: McGraw Hill.

[2] Central Station Engineers of Westinghouse Electric Corporation. 1950. Electrical transmission and distribution reference book. Pennsylvania, USA.

[3] Alsac, O. and Stott, B. 1974. Optimal load flow with steady state security. IEEE Transactions on Power Apparatus and Systems 93: 745-51.

[4] Shoults, R.R. and Sun, D.T. 1982. Optimal power flow based on P-Q decomposition. IEEE Transactions on Power Apparatus and Systems 101: 397-405.

[5] Bottero, M.H.; Galiana, F.D.; and Fahmideh Vojdani, A.R. 1982. Economic dispatch using the reduced Hessian. IEEE Transactions on Power Apparatus and Systems 101:3679-88.

[6] Momoh, J.A. 1989. Generalized quadratic-based model for optimal power flow. IEEE international conference on systems, man and cybernetics. Cambridge, USA, 14-17 November, p. 261-71.

[7] Momoh, J.A.; El-Hawary, M.E.; and Adapa, R. 1999. A review of selected optimal power flow literature to 1993. Part I: Nonlinear and quadratic programming approaches. IEEE Transactions on Power Systems 14(1): 96-104.

[8] Stott, B. and Hobson, E. 1978. Power system security control calculation using linear programming. IEEE Transactions on Power Apparatus and Systems 97:1713-31.

[9] Stott, B. and Marinho, J.L. 1979. Linear programming for power system network security applications. IEEE Transactions on Power Apparatus and Systems 98: 837-48.

[10] Mota-Palomino, R and Quintana, V.H. 1984. A penalty function-linear programming method for solving power system constrained economic operation problems. IEEE Transactions on Power Apparatus and Systems 103: 1414-42.

[11] Momoh, J.A.; Hawary, M.E.; and Adapa, R. 1999. A review of selected optimal power flow literature to 1993. Part II: Newton, linear programming and interior point methods. IEEE Transactions on Power Systems 14(1): 105-11.

[12] Abido, M.A. 2002. Optimal power flow using particle swarm optimization. Internal Journal of Electrical Power and Energy Systems 24(7): 563-571.

[13] Attous, D.B. and Labbi, Y. 2009. Particle swarm optimization based optimal power flow for units with non-smooth fuel cost functions. International Conference on IEEE Electrical and Electronics Engineering (ELECO 2009), Bursa, Turkey, 05-08 November.

[14] Niknam, T.; Narimani, M.R.; Aghaei, J.; and Azizipanah-Abarghooee, R. 2012. Improved particle swarm optimisation for multi-objective optimal power flow considering the cost, loss, emission and voltage stability index. IET Generation, Transmission and Distribution 6(6): 515-527.

[15] Younis, U.; Khaliq, A.; and Saleem, M. 2018. Weights aggregated multiobjective particle swarm optimizer for optimal power flow considering the generation cost, emission, transmission loss and bus voltage profile. International Journal of Innovative Computing, Information and Control 14(4):1423-1441.

[16] Roberge, V.; Tarbouchi, M.; and Okou, F. 2016. Optimal power flow based on parallel metaheuristics for graphics processing units. Electric Power Systems Research 140: 344-353.

[17] Vo, D.N. and Schegner, P. An improved particle swarm optimization for optimal power flow. In: Meta-heuristics optimization algorithms in engineering, business, economics, and finance. IGI Global 2013, pp 1–40.

[18] Vaisakh, K.; Srinivas, L.R.; and Meah, K. 2013. Genetic evolving ant direction particle swarm optimization algorithm for optimal power flow with non-smooth cost functions and statistical analysis. Applied Soft Computing 13(12): 4579-4593.

[19] El-Fergany, A.A. and Hasanien, H.M. 2015. Single and multi-objective optimal power flow using grey wolf optimizer and differential evolution algorithms. Electric Power Component and Systems 43(13): 1548-1559.

[20] El Ela, A.A.; Abido, M.A.; and Spea, S.R. 2010. Optimal power flow using differential evolution algorithm. Electric Power Systems Research 80(7): 878-885.

[21] Sayah, S. and Zehar, K. 2008. Modified differential evolution algorithm for optimal power flow with non-smooth cost functions. Energy Conversion and Management 49(11): 3036-3042.

[22] Al-Attar Ali Mohamed; Yahia S. Mohamed; Ahmed A.M. El-Gaafary; and Ashraf M. Hemeida. 2017. Optimal power flow using moth swarm algorithm. Electric Power Systems Research 142: 190-206.

[23] Adaryani, M.R. and Karami, A. 2013. Artificial bee colony algorithm for solving multi-objective optimal power flow problem. International Journal of Electrical Power and Energy Systems 53: 219-230.

[24] Yuryevich, J. and Wong, K.P. 1999. Evolutionary programming based optimal power flow algorithm. IEEE Transactions on Power Systems 14(4): 1245-50.

[25] Kumar, A.R. and Premalatha, L. 2015. Optimal power flow for a deregulated power system using adaptive real coded biogeography-based optimization. International Journal of Electrical Power and Energy Systems 73:393-399.

[26] El-Fergany, A.A. and Hasanien, H.M. 2015. Single and multi-objective optimal power flow using grey wolf optimizer and differential evolution algorithms. Electric Power Components and Systems 43(13): 1548-1559.

[27] Chen, G.; Lu, Z.; and Zhang, Z. 2018. Improved krill herd algorithm with novel constraint handling method for solving optimal power flow problems. Energies 11(1): 1-27.

[28] Abido, M.A. 2002. Optimal power flow using tabu search algorithm. Electric Power Components and Systems 30(5): 469-83.

[29] Ghasemi, M.; Ghavidel, S.; Ghanbarian, M.M.; and Gitizadeh, M. 2015. Multi-objective optimal electric power planning in the power system using Gaussian bare-bones imperialist competitive algorithm, Information Science 294: 286-304.

[30] Taher, M.A.; Kamel, S.; Jurado, F.; and Ebeed, M.. 2018. An improved moth-flame optimization algorithm for solving optimal power flow problem. International Transactions on Electrical Energy Systems 29(3): 1-28.

[31] Pandiarajan, K. and Babulal, C. 2016. Fuzzy harmony search algorithm based optimal power flow for power system security enhancement. International Journal of Electrical Power and Energy Systems 78: 72-79.

[32] Chaib, A.E; Bouchekara, H.R.E.H.; Mehasni. R; and Abido, M.A. Optimal power flow with emission and non-smooth cost functions using backtracking search optimization

algorithm. Electrical Power and Energy Systems 81: 64-77.
[33] Bouchekara, H.R.E.H; Chaib, A.E; Abido, M.A; and El-Sehiemy, R.A. 2016. Optimal power flow using an improved colliding bodies optimization algorithm. Applied Soft Computing 42: 119-131.
[34] El-Fergany, A.A. and Hasanien, H.M. 2020. Salp swarm optimizer to solve optimal power flow comprising voltage stability analysis. Neural Computing and Applications 32: 5267-5283.
[35] Naderi, E; Pourakbari-Kasmaei, M.; Cerna, F.V.; and Lehtonen, M. 2021. A novel hybrid self-adaptive heuristic algorithm to handle single and multiobjective optimal power flow problems. International Journal of Electrical Power and Energy Systems 125: 1-16.
[36] Le, D.L.; Ho, D.L; and V, N.D. 2015. Improved Particle swarm optimization method for optimal power flow with FACTS devices. GMSARN International Journal 9: 37-55.
[37] Duong, M.P.; Vo, N.D; Nguyen, T.T; and Phan, V.D. 2015. Optimal power flow in power system considering wind power integrated into grid. GMSARN International Journal 9: 37-55.
[38] Cecchi, V. 2010. Temperature-dependent transmission line models for electric power systems and their impacts on system studies. PhD dissertation, Drexel University.
[39] Frank, S.; Sexauer, J.; and Mohagheghi, S. 2013. Temperature-Dependent Power Flow, IEEE Transactions on Power Systems 28(4): 4007-4018.
[40] Rahman, M.; Cecchi, V.; and Miu, K. 2019. Power handling capabilities of transmission systems using a temperature dependent power flow. Electric Power Systems Research 169: 241-249.
[41] Gao, Q.; Wei, Z.; Sun, Q.; Sun, Y.; and Zhang, H. 2015. Temperature-dependent optimal power flow based on simplified interior point method. The 5th International Conference on Electric Utility Deregulation and Restructuring and Power Technologies (DRPT), Changsha, China, 26-29 November, p. 765-769.
[42] Jadhav, H.T. and Bamane, P.D. 2016. Temperature dependent optimal power flow using g-best guided artificial bee colony algorithm. Electrical Power and Energy Systems 77: 77-90.
[43] Ghosh, A. and Mukherjee, V. 2017. Temperature dependent optimal power flow. The 2017 IEEE International Conference on Technological Advancements in Power and Energy (TAP Energy), Kollam , India, 21-23 December, 6 pages.
[44] Picanco, A.F. and Oliveira, A.P. 2018. Reactive optimal power flow in the temperature-dependent power flow using interior point method with artificial neural network. Mediterranean Conference on Power Generation, Transmission, Distribution and Energy Conversion (MEDPOWER 2018), Dubrovnik, Croatia, 12-15 November, 6 pages.
[45] Prasad, D.; Mukherjee, A.; and Mukherjee,V. 2021. Temperature dependent optimal power flow using chaotic whale optimization algorithm. Expert Systems e12685: 1-14.
[46] Picanco, A.F.; de Oliveira, A.S.A.; Moreira, F.A.; and Santos, E.T.F. 2021. Optimal temperature-dependent power flow using quantum-behaved particle swarm optimization. The 19th International Conference on Smart Technologies (IEEE EUROCON 2021), Lviv, Ukraine, 06-08 July, p. 414-419.
[47] IEEE Std. C57.12.91-2001. 1996. C57.12.91-1995 - IEEE Standard Test Code for Dry-Type Distribution and Power Transformers, IEEE Publisher.
[48] Glover, J.D.; Sarma, M.S.; and Overbye, T.J. 2008. Power System Analysis and Design. 4th ed. Stamford, CT: Cengage Learning.
[49] IEEE Std. 399. 1997. IEEE Recommended practice for industrial and commercial power systems analysis (Brown book). IEEE Publisher.
[50] Banakar, H.; Alguacil, N.; and Galiana, F.D. 2005. Electrothermal coordination part I: Theory and implementation schemes. IEEE Transactions on Power Systems 20(2): 798-805.
[51] Kennedy, J and Eberhart, R. 1995. Particle swarm optimization. Proceedings of the IEEE International Conference on Neural Networks, Perth, Australia, 27 November - 01 December pp.1942-1948.
[52] Storn, R. and Price, K. 1997. Differential evolution - A simple and efficient heuristic for global optimization over continuous spaces. Journal of Global Optimization 11: 341-359.
[53] Zimmerman, R.D.; Murillo-Sánchez, C.E.; and Thomas, R.J. 2011. Matpower: Steady-State Operations, Planning and Analysis Tools for Power Systems Re-search and Education. IEEE Transactions on Power Systems 26(1): 12-19.

APPENDIX

Table A.1. The control parameters of CPSO-DE, PSO, and DE algorithms for the IEEE 30-bus test system

Parameter	CPSO-DE	PSO	DE
N_p	50	50	50
$iter_{max}$	100	100	100
c_1	2	2	-
c_2	2	2	-
ω	0.8	0.8	-
F	0.6	-	0.6
CR	0.9	-	0.9
R	0.02	0.02	-

Table A.2. The optimal solution by the proposed CPSO-DE in the conventional OPF problem for the IEEE 30-bus system

Control variables	Value	Control variables	Value
P_{g2} (MW)	48.73314281	Q_{c15} (MVAr)	3.52141682
P_{g5} (MW)	21.35930373	Q_{c17} (MVAr)	4.85375734
P_{g8} (MW)	21.20182901	Q_{c20} (MVAr)	4.11343274
P_{g11} (MW)	11.92441013	Q_{c21} (MVAr)	4.89443506
P_{g13} (MW)	12.01257730	Q_{c23} (MVAr)	3.37161548
V_{g1} (pu)	1.082036941	Q_{c24} (MVAr)	4.86458281

V_{g2} (pu)	1.063484023	Q_{c29} (MVAr)	2.21078133
V_{g5} (pu)	1.032167830	T_{6-9} (pu)	1.01441682
V_{g8} (pu)	1.036732029	T_{6-10} (pu)	0.94975349
V_{g11} (pu)	1.062570745	T_{4-12} (pu)	0.97832438
V_{g13} (pu)	1.047330539	T_{28-27} (pu)	0.97147248
Q_{c10} (MVAr)	4.910600075	Fuel cost ($/h)	800.435313
Q_{c12} (MVAr)	4.86519437	P_{loss} (MW)	9.01340750
		P_{slack} (MW)	177.182144

Table A.3. The optimal solution by the proposed CPSO-DE in the TDOPF problem for the IEEE 30-bus system with the temperature rise of 25°C

Control variables	Value	Control variables	Value
P_{g2} (MW)	48.90839	Q_{c12} (MVAr)	3.606704
P_{g5} (MW)	21.65961	Q_{c15} (MVAr)	4.184024
P_{g8} (MW)	21.75972	Q_{c17} (MVAr)	4.36245
P_{g11} (MW)	12.13954	Q_{c20} (MVAr)	3.265375
P_{g13} (MW)	12.01667	Q_{c21} (MVAr)	4.919097
V_{g1} (pu)	1.093115	Q_{c23} (MVAr)	4.303744
V_{g2} (pu)	1.073456	Q_{c24} (MVAr)	3.896
V_{g5} (pu)	1.042182	Q_{c29} (MVAr)	2.501176
V_{g8} (pu)	1.046714	T_{6-9} (pu)	0.992415
V_{g11} (pu)	1.061485	T_{6-10} (pu)	0.970375
V_{g13} (pu)	1.060757	T_{4-12} (pu)	0.980508
Q_{c10} (MVAr)	3.408454	T_{28-27} (pu)	0.97296
Fuel cost ($/h)		800.8220	
P_{loss} (MW)		9.0237	
P_{slack} (MW)		175.9398	

Table A.4. The resistance difference in branches for 250C temperature rise in the TDOPF problem for the IEEE 30-bus system

Branch no.	From	To	PF	TDOPF	Relative difference (%)
1	1	2	0.0192	0.02043367	6.425407
2	1	3	0.0452	0.04585745	1.454539
3	2	4	0.057	0.05821105	2.124664
4	3	4	0.0132	0.01345898	1.961991
5	2	5	0.0472	0.0480626	1.827707
6	2	6	0.0581	0.06034427	3.862773
7	4	6	0.0119	0.01226139	3.036967
8	5	7	0.046	0.04610028	0.218002
9	6	7	0.0267	0.02684100	0.528101
10	6	8	0.012	0.01220396	1.699674
11	6	9	0	0	0
12	6	10	0	0	0
13	9	11	0	0	0
14	9	10	0	0	0
15	4	12	0	0	0
16	12	13	0	0	0
17	12	14	0.1231	0.12368078	0.471802
18	12	15	0.0662	0.06781009	2.432175
19	12	16	0.0945	0.09486901	0.390489
20	14	15	0.221	0.22116546	0.074872
21	16	17	0.0824	0.08270539	0.370623
22	15	18	0.1073	0.10840454	1.029399
23	18	19	0.0639	0.06403853	0.216792
24	19	20	0.034	0.03415971	0.469738
25	10	20	0.0936	0.09429941	0.747243
26	10	17	0.0324	0.03249629	0.297215
27	10	21	0.0348	0.03566777	2.493614
28	10	22	0.0727	0.07306739	0.505355
29	21	22	0.0116	0.01160342	0.02956
30	15	23	0.1	0.10086886	0.86887
31	22	24	0.115	0.11630191	1.132103
32	23	24	0.132	0.13211574	0.087689
33	24	25	0.1885	0.18863886	0.073668
34	25	26	0.2544	0.25545220	0.413604
35	25	27	0.1093	0.11016908	0.795136
36	28	27	0	0	0
37	27	29	0.2198	0.22260310	1.275297
38	27	30	0.3202	0.32544085	1.636743
39	29	30	0.2399	0.24101200	0.463531
40	8	28	0.0636	0.06366400	0.100636
41	6	28	0.0169	0.01720423	1.800187

Table A.5. The control parameters of CPSO-DE, PSO, and DE algorithms for the IEEE 118-bus test system

Parameter	CPSO-DE	DE	PSO
N_p	75	75	75
$iter_{max}$	300	300	300
c_1	2	-	2
c_2	2	-	2
ω	0.8	-	0.8
F	0.6	0.6	-
CR	0.9	0.9	-
R	0.02	-	0.02

Table A.6. The optimal solution by the proposed CPSO-DE in the conventional OPF problem for the IEEE 118-bus system

Control variable	Value	Control variable	Value	Control variable	Value
P_{g1} (MW)	30.6299	P_{g103} (MW)	38.1213	V_{g77} (pu)	1.0304
P_{g4} (MW)	1.0874	P_{g104} (MW)	0.5086	V_{g80} (pu)	1.0503
P_{g6} (MW)	0.0552	P_{g105} (MW)	11.2697	V_{g85} (pu)	1.0213
P_{g8} (MW)	0.0121	P_{g107} (MW)	25.6520	V_{g87} (pu)	1.0246
P_{g10} (MW)	401.0669	P_{g110} (MW)	8.7079	V_{g89} (pu)	1.0387
P_{g12} (MW)	85.4522	P_{g111} (MW)	36.5486	V_{g90} (pu)	1.0136
P_{g15} (MW)	18.5857	P_{g112} (MW)	39.6947	V_{g91} (pu)	1.0216
P_{g18} (MW)	13.1349	P_{g113} (MW)	0.5737	V_{g92} (pu)	1.0276
P_{g19} (MW)	21.1157	P_{g116} (MW)	0.6740	V_{g99} (pu)	1.0394
P_{g24} (MW)	0.1115	V_{g1} (pu)	1.0098	V_{g100} (pu)	1.0381
P_{g25} (MW)	194.8113	V_{g4} (pu)	1.0350	V_{g103} (pu)	1.0298
P_{g26} (MW)	281.9627	V_{g6} (pu)	1.0311	V_{g104} (pu)	1.0120
P_{g27} (MW)	12.2253	V_{g8} (pu)	1.0289	V_{g105} (pu)	1.0063
P_{g31} (MW)	7.3672	V_{g10} (pu)	1.0414	V_{g107} (pu)	0.9878
P_{g32} (MW)	12.9233	V_{g12} (pu)	1.0294	V_{g110} (pu)	1.0170
P_{g34} (MW)	3.3962	V_{g15} (pu)	1.02807	V_{g111} (pu)	1.0250
P_{g36} (MW)	3.5608	V_{g18} (pu)	1.03093	V_{g112} (pu)	1.0159
P_{g40} (MW)	49.8937	V_{g19} (pu)	1.02852	V_{g113} (pu)	1.0445
P_{g42} (MW)	40.6650	V_{g24} (pu)	1.0491	V_{g116} (pu)	1.0086
P_{g46} (MW)	17.5645	V_{g25} (pu)	1.0582	Q_{c5} (MVAr)	0.4502
P_{g49} (MW)	192.5920	V_{g26} (pu)	1.0536	Q_{c34} (MVAr)	0.1154
P_{g54} (MW)	49.3221	V_{g27} (pu)	1.0497	Q_{c37} (MVAr)	0.0207
P_{g55} (MW)	29.4698	V_{g31} (pu)	1.0407	Q_{c44} (MVAr)	1.2862
P_{g56} (MW)	36.7466	V_{g32} (pu)	1.0435	Q_{c45} (MVAr)	4.7030
P_{g59} (MW)	149.6279	V_{g34} (pu)	1.0450	Q_{c46} (MVAr)	3.1860
P_{g61} (MW)	148.6880	V_{g36} (pu)	1.0426	Q_{c48} (MVAr)	3.8094
P_{g62} (MW)	0	V_{g40} (pu)	1.0210	Q_{c74} (MVAr)	3.9307
P_{g65} (MW)	352.3260	V_{g42} (pu)	1.0148	Q_{c79} (MVAr)	0.1570

P_{g66} (MW)	351.3875	V_{g46} (pu)	1.0225	Q_{c82} (MVAr)	2.5184
P_{g70} (MW)	0.0647	V_{g49} (pu)	1.0372	Q_{c83} (MVAr)	3.2868
P_{g72} (MW)	0.0402	V_{g54} (pu)	1.0213	Q_{c105} (MVAr)	0.6844
P_{g73} (MW)	0.0571	V_{g55} (pu)	1.0183	Q_{c107} (MVAr)	1.6332
P_{g74} (MW)	15.2900	V_{g56} (pu)	1.0189	Q_{c110} (MVAr)	0.3811
P_{g76} (MW)	28.6599	V_{g59} (pu)	1.0253	T_{8-5}	0.9915
P_{g77} (MW)	0.0471	V_{g61} (pu)	1.0416	T_{26-25}	1.0191
P_{g80} (MW)	430.9242	V_{g62} (pu)	1.0377	T_{30-17}	1.0092
P_{g85} (MW)	0.0433	V_{g65} (pu)	1.0361	T_{38-37}	0.9556
P_{g87} (MW)	3.8517	V_{g66} (pu)	1.0416	T_{63-59}	1.0320
P_{g89} (MW)	501.9555	V_{g69} (pu)	1.0509	T_{64-61}	0.9884
P_{g90} (MW)	0.0359	V_{g70} (pu)	1.0190	T_{65-66}	1.0080
P_{g91} (MW)	0.0548	V_{g72} (pu)	1.0396	T_{68-69}	0.9816
P_{g92} (MW)	0.5454	V_{g73} (pu)	1.0178	T_{70-71}	0.9751
P_{g99} (MW)	0.5563	V_{g74} (pu)	0.9948		
P_{g100} (MW)	220.5270	V_{g76} (pu)	0.9924		
Fuel cost ($/h)			129796.169		
P_{loss} (MW)			80.2349		
P_{slack} (MW)			452.0475		

Table A.7. The optimal solution by the proposed CPSO-DE in the TDOPF problem for the IEEE 118-bus system with the temperature rise of 250C

Control variable	Value	Control variable	Value	Control variable	Value
P_{g1} (MW)	25.7631	P_{g103} (MW)	37.2384	V_{g77}(pu)	1.0288
P_{g4} (MW)	1.3256	P_{g104} (MW)	1.8052	V_{g80}(pu)	1.0529
P_{g6} (MW)	1.5787	P_{g105} (MW)	5.8617	V_{g85}(pu)	1.0082
P_{g8} (MW)	1.2296	P_{g107} (MW)	28.2478	V_{g87}(pu)	1.0058
P_{g10} (MW)	401.4343	P_{g110} (MW)	7.8972	V_{g89}(pu)	1.0282
P_{g12} (MW)	85.7002	P_{g111} (MW)	34.9499	V_{g90}(pu)	1.0308
P_{g15} (MW)	20.910	P_{g112} (MW)	35.9154	V_{g91} (pu)	1.0398
P_{g18} (MW)	12.1952	P_{g113} (MW)	1.0716	V_{g92} (pu)	1.0228
P_{g19} (MW)	21.8435	P_{g116} (MW)	1.8061	V_{g99} (pu)	1.0229
P_{g24} (MW)	1.1894	V_{g1} (pu)	0.9932	V_{g100} (pu)	1.0360
P_{g25} (MW)	192.7152	V_{g4} (pu)	1.0326	V_{g103} (pu)	1.0293
P_{g26} (MW)	278.4323	V_{g6} (pu)	1.0178	V_{g104} (pu)	1.0209
P_{g27} (MW)	9.2948	V_{g8} (pu)	1.0385	V_{g105} (pu)	1.0212
P_{g31} (MW)	6.7389	V_{g10} (pu)	1.0336	V_{g107} (pu)	1.0463

P_{g32} (MW)	14.0845	V_{g12} (pu)	1.0194	V_{g110} (pu)	1.0179
P_{g34} (MW)	5.3929	V_{g15} (pu)	1.0191	V_{g111} (pu)	1.0327
P_{g36} (MW)	9.5964	V_{g18} (pu)	1.0230	V_{g112} (pu)	1.0074
P_{g40} (MW)	48.2025	V_{g19} (pu)	1.0181	V_{g113} (pu)	1.0482
P_{g42} (MW)	40.6905	V_{g24} (pu)	1.0259	V_{g116} (pu)	1.0213
P_{g46} (MW)	18.2240	V_{g25} (pu)	1.0380	Q_{c5} (MVAr)	4.1280
P_{g49} (MW)	192.6964	V_{g26} (pu)	1.0270	Q_{c34} (MVAr)	-10.8799
P_{g54} (MW)	49.6978	V_{g27} (pu)	1.0194	Q_{c37} (MVAr)	2.8466
P_{g55} (MW)	32.7158	V_{g31} (pu)	1.0050	Q_{c44} (MVAr)	-14.9920
P_{g56} (MW)	31.8982	V_{g32} (pu)	1.0145	Q_{c45} (MVAr)	-3.3721
P_{g59} (MW)	148.8603	V_{g34} (pu)	1.0350	Q_{c46} (MVAr)	-12.7190
P_{g61} (MW)	147.9663	V_{g36} (pu)	1.0341	Q_{c48} (MVAr)	2.3262
P_{g62} (MW)	1.6034	V_{g40} (pu)	1.0173	Q_{c74} (MVAr)	14.0724
P_{g65} (MW)	353.0448	V_{g42} (pu)	1.0236	Q_{c79} (MVAr)	-1.4608
P_{g66} (MW)	348.3026	V_{g46} (pu)	1.0340	Q_{c82} (MVAr)	0.3659
P_{g70} (MW)	1.9474	V_{g49} (pu)	1.0430	Q_{c83} (MVAr)	16.5073
P_{g72} (MW)	0.9042	V_{g54} (pu)	1.0226	Q_{c105} (MVAr)	-3.0656
P_{g73} (MW)	1.1883	V_{g55} (pu)	1.0184	Q_{c107} (MVAr)	8.2513
P_{g74} (MW)	16.2106	V_{g56} (pu)	1.0190	Q_{c110} (MVAr)	-1.7496
P_{g76} (MW)	22.5001	V_{g59} (pu)	1.0184	T_{8-5}	0.9879
P_{g77} (MW)	2.1456	V_{g61} (pu)	1.0388	T_{26-25}	1.0268
P_{g80} (MW)	430.9408	V_{g62} (pu)	1.0330	T_{30-17}	1.0422
P_{g85} (MW)	1.7732	V_{g65} (pu)	1.0490	T_{38-37}	0.9694
P_{g87} (MW)	1.7700	V_{g66} (pu)	1.0451	T_{63-59}	1.0087
P_{g89} (MW)	501.4367	V_{g69} (pu)	1.0476	T_{64-61}	0.9942
P_{g90} (MW)	1.3511	V_{g70} (pu)	1.0145	T_{65-66}	1.0194
P_{g91} (MW)	1.6585	V_{g72} (pu)	1.0397	T_{68-69}	0.9441
P_{g92} (MW)	1.5981	V_{g73} (pu)	1.0186	T_{70-71}	0.9707
P_{g99} (MW)	1.2326	V_{g74} (pu)	0.9984		
P_{g100} (MW)	230.2928	V_{g76} (pu)	0.9825		
Fuel cost ($/h)			129960.315		
P_{loss} (MW)			84.1887		
P_{slack} (MW)			451.1151		

Table A.8. The resistance difference in branches for 25^{o}C temperature rise in the TDOPF problem for the IEEE 118-bus system

Branch number	From	To	PF	TDOPF	Relative difference (%)
1	1	2	0.0303	0.03031	0.033944
2	1	3	0.0129	0.01293	0.232694
3	4	5	0.00176	0.00177	0.316209
4	3	5	0.0241	0.02433	0.975006
5	5	6	0.0119	0.01212	1.887922
6	6	7	0.00459	0.0046	0.254335
7	8	9	0.00244	0.00257	5.459195
8	8	5	0	0	0
9	9	10	0.00258	0.00273	5.86197
10	4	11	0.0209	0.0211	0.949555
11	5	11	0.0203	0.02058	1.372458
12	11	12	0.00595	0.00597	0.268896
13	2	12	0.0187	0.01875	0.247344
14	3	12	0.0484	0.04841	0.028523
15	7	12	0.00862	0.00862	0.046184
16	11	13	0.02225	0.02232	0.306399
17	12	14	0.0215	0.02151	0.068448
18	13	15	0.0744	0.07441	0.009045
19	14	15	0.0595	0.0595	0.000553
20	12	16	0.0212	0.0212	0.023576
21	15	17	0.0132	0.01323	0.224864
22	16	17	0.0454	0.04544	0.079835
23	17	18	0.0123	0.01243	1.058049
24	18	19	0.01119	0.0112	0.063857
25	19	20	0.0252	0.02521	0.026818
26	15	19	0.012	0.012	0.005274
27	20	21	0.0183	0.01833	0.139672
28	21	22	0.0209	0.02097	0.34264
29	22	23	0.0342	0.0344	0.570816
30	23	24	0.0135	0.01351	0.087752
31	23	25	0.0156	0.01572	0.746448
32	26	25	0	0	0
33	25	27	0.0318	0.03197	0.525448
34	27	28	0.01913	0.01918	0.277177
35	28	29	0.0237	0.02371	0.051784
36	30	17	0	0	0
37	8	30	0.00431	0.00438	1.588164

38	26	30	0.00799	0.0081	1.389124
39	17	31	0.0474	0.04746	0.135988
40	29	31	0.0108	0.0108	0.033962
41	23	32	0.0317	0.03254	2.641076
42	31	32	0.0298	0.02987	0.226428
43	27	32	0.0229	0.02291	0.028756
44	15	33	0.038	0.03801	0.014976
45	19	34	0.0752	0.07521	0.013508
46	35	36	0.00224	0.00224	0.001434
47	35	37	0.011	0.01103	0.282928
48	33	37	0.0415	0.04154	0.105098
49	34	36	0.00871	0.00872	0.158049
50	34	37	0.00256	0.00257	0.364703
51	38	37	0	0	0
52	37	39	0.0321	0.03221	0.350811
53	37	40	0.0593	0.0594	0.166835
54	30	38	0.00464	0.0047	1.251003
55	39	40	0.0184	0.0184	0.013047
56	40	41	0.0145	0.01452	0.117139
57	40	42	0.0555	0.05551	0.016581
58	41	42	0.041	0.04104	0.088569
59	43	44	0.0608	0.06084	0.059295
60	34	43	0.0413	0.04134	0.089495
61	44	45	0.0224	0.02244	0.182432
62	45	46	0.04	0.04016	0.406214
63	46	47	0.038	0.03808	0.207649
64	46	48	0.0601	0.06014	0.060986
65	47	49	0.0191	0.01912	0.08402
66	42	49	0.0715	0.07183	0.462157
67	42	49	0.0715	0.07183	0.462157
68	45	49	0.0684	0.06884	0.639144
69	48	49	0.0179	0.01796	0.328481
70	49	50	0.0267	0.02685	0.565409
71	49	51	0.0486	0.04903	0.887419
72	51	52	0.0203	0.02034	0.195092
73	52	53	0.0405	0.04051	0.019225
74	53	54	0.0263	0.02632	0.090976
75	49	54	0.073	0.07319	0.266995
76	49	54	0.0869	0.08712	0.257152

77	54	55	0.0169	0.0169	0.009543
78	54	56	0.00275	0.00276	0.401437
79	55	56	0.00488	0.00488	0.009277
80	56	57	0.0343	0.03432	0.07242
81	50	57	0.0474	0.0475	0.219857
82	56	58	0.0343	0.0343	0.010157
83	51	58	0.0255	0.02551	0.050938
84	54	59	0.0503	0.05038	0.150199
85	56	59	0.0825	0.08259	0.114143
86	56	59	0.0803	0.0804	0.125354
87	55	59	0.04739	0.04747	0.167647
88	59	60	0.0317	0.03182	0.392474
89	59	61	0.0328	0.03299	0.58958
90	60	61	0.00264	0.00265	0.399533
91	60	62	0.0123	0.0123	0.019941
92	61	62	0.00824	0.00826	0.246465
93	63	59	0	0	0
94	63	64	0.00172	0.00173	0.583136
95	64	61	0	0	0
96	38	65	0.00901	0.00907	0.615079
97	64	65	0.00269	0.00272	0.934785
98	49	66	0.018	0.01807	0.37063
99	49	66	0.018	0.01807	0.37063
100	62	66	0.0482	0.04835	0.313819
101	62	67	0.0258	0.02583	0.120854
102	65	66	0	0	0
103	66	67	0.0224	0.02255	0.653199
104	65	68	0.00138	0.00139	0.792472
105	47	69	0.0844	0.08488	0.572191
106	49	69	0.0985	0.09885	0.356664
107	68	69	0	0	0
108	69	70	0.03	0.03009	0.291722
109	24	70	0.00221	0.00221	0.002417
110	70	71	0.00882	0.00883	0.09824
111	24	72	0.0488	0.04882	0.031829
112	71	72	0.0446	0.04462	0.053496
113	71	73	0.00866	0.00866	0.006584
114	70	74	0.0401	0.04013	0.076462
115	70	75	0.0428	0.04281	0.023408

116	69	75	0.0405	0.04063	0.317142
117	74	75	0.0123	0.01235	0.425989
118	76	77	0.0444	0.0447	0.665984
119	69	77	0.0309	0.03132	1.345437
120	75	77	0.0601	0.06021	0.177414
121	77	78	0.00376	0.0038	0.944634
122	78	79	0.00546	0.00547	0.129148
123	77	80	0.017	0.01704	0.264549
124	77	80	0.0294	0.02942	0.058678
125	79	80	0.0156	0.0158	1.250179
126	68	81	0.00175	0.00175	0.014297
127	81	80	0	0	0
128	77	82	0.0298	0.02984	0.147428
129	82	83	0.0112	0.01121	0.115457
130	83	84	0.0625	0.06256	0.091996
131	83	85	0.043	0.0431	0.234355
132	84	85	0.0302	0.03026	0.200963
133	85	86	0.035	0.035	0.013643
134	86	87	0.02828	0.02828	0.000588
135	85	88	0.02	0.02008	0.41225
136	85	89	0.0239	0.02413	0.975016
137	88	89	0.0139	0.01394	0.259285
138	89	90	0.0518	0.05186	0.106477
139	89	90	0.0238	0.02389	0.386357
140	90	91	0.0254	0.02541	0.036803
141	89	92	0.0099	0.00998	0.78241
142	89	92	0.0393	0.03933	0.077564
143	91	92	0.0387	0.03876	0.16565
144	92	93	0.0258	0.02591	0.433525
145	92	94	0.0481	0.04826	0.322606
146	93	94	0.0223	0.02235	0.220266
147	94	95	0.0132	0.01326	0.465204
148	80	96	0.0356	0.03569	0.26222
149	82	96	0.0162	0.01621	0.074968
150	94	96	0.0269	0.02692	0.077555
151	80	97	0.0183	0.01838	0.413008
152	80	98	0.0238	0.02385	0.221977
153	80	99	0.0454	0.04544	0.093603
154	92	100	0.0648	0.06485	0.074903

155	94	100	0.0178	0.01788	0.452525
156	95	96	0.0171	0.01711	0.082804
157	96	97	0.0173	0.01732	0.142104
158	98	100	0.0397	0.03971	0.013636
159	99	100	0.018	0.01803	0.182436
160	100	101	0.0277	0.02772	0.062257
161	92	102	0.0123	0.01233	0.219867
162	101	102	0.0246	0.02464	0.149002
163	100	103	0.016	0.01603	0.182554
164	100	104	0.0451	0.04529	0.424811
165	103	104	0.0466	0.04668	0.175199
166	103	105	0.0535	0.05364	0.261316
167	100	106	0.0605	0.0608	0.487851
168	104	105	0.00994	0.00996	0.228144
169	105	106	0.014	0.01401	0.036541
170	105	107	0.053	0.05307	0.13169
171	105	108	0.0261	0.0261	0.017863
172	106	107	0.053	0.05306	0.105787
173	108	109	0.0105	0.0105	0.0104
174	103	110	0.03906	0.03917	0.272105
175	109	110	0.0278	0.0278	0.001325
176	110	111	0.022	0.02208	0.36775
177	110	112	0.0247	0.02477	0.30248
178	17	113	0.00913	0.00924	1.166608
179	32	113	0.0615	0.06151	0.00986
180	32	114	0.0135	0.0135	0.036098
181	27	115	0.0164	0.01642	0.113328
182	114	115	0.0023	0.0023	0.002708
183	68	116	0.00034	0.00035	1.666898
184	12	117	0.0329	0.03294	0.127844
185	75	118	0.0145	0.01457	0.49083
186	76	118	0.0164	0.0164	0.013192